The Iso-Competition Point for Counterion Competition Binding to DNA: Calculated Multivalent Versus Monovalent Cation Binding Equivalence

Anzhi Z. Li and Kenneth A. Marx
Department of Chemistry, University of Massachusetts Lowell, Lowell, Massachusetts 01854 USA

ABSTRACT In this paper we introduce an important parameter called the iso-competition point (ICP), to characterize the competition binding to DNA in a two-cation-species system. By imposing the condition of charge neutralization fraction equivalence $\theta_1 = Z\theta_Z$ upon the two simultaneous equations in Manning's counterion condensation theory, the ICPs can be calculated. Each ICP, which refers to a particular multivalent concentration where the charge fraction on DNA neutralized from monovalent cations equals that from the multivalent cations, corresponds to a specific ionic strength condition. At fixed ionic strength, the total DNA charge neutralization fractions θ_{ICP} are equal, no matter whether the higher valence cation is divalent, trivalent, or tetravalent. The ionic strength effect on ICP can be expressed by a semiquantitative equation as $ICP_{Za}/ICP_{Zb} = (I_a/I_b)^Z$, where I_a, I_b refers to the instance of ionic strengths and Z indicates the valence. The ICP can be used to interpret and characterize the ionic strength, valence, and DNA length effects on the counterion competition binding in a two-species system. Data from our previous investigations involving binding of Mg^{2+}, Ca^{2+}, and $Co(NH_3)_6^{3+}$ to λ-DNA-*Hind*III fragments ranging from 2.0 to 23.1 kbp was used to investigate the applicability of ICP to describe counterion binding. It will be shown that the ICP parameter presents a prospective picture of the counterion competition binding to polyelectrolyte DNA under a specific ion environment condition.

INTRODUCTION

For over two decades, the phenomenon of counterion condensation has attracted many scientists' experimental and theoretical attention, either from a biological view or polyelectrolyte perspective. Particularly from the standpoint of conformational properties of polyion DNA, such as the helix-coil transition (Widom and Baldwin, 1980; Bloomfield, 1991), the condensation based collapse of DNA and its resulting structure (Allison et al., 1981; Marx and Ruben, 1983, 1986; Marx and Reynolds, 1982, 1989; Arscott et al., 1990; Plum et al., 1990; Li et al., 1992), has been fairly well studied. A variety of experimental approaches, including NMR (Granot and Kearns, 1982), differential scanning calorimetry (Labarbe et al., 1996), Raman spectroscopy (Langlais et al., 1990), absorption measurements (Manzini et al., 1990), electrophoretic light scattering (Rhee and Ware, 1983; Xia et al., 1993), and gel electrophoresis (Ma and Bloomfield, 1995; Li et al., 1996, 1998) have been employed to measure the counterion binding to DNA. These studies compared the experimental results with predictions from polyelectrolyte theory, either Manning's counterion condensation (CC) theory (Manning, 1977, 1978, 1981), and/or the Poisson-Boltzmann (PB) equation.

Our previous studies were focused on the counterion competition binding of multivalent versus monovalent counterions onto polyelectrolyte DNA. The interactions of divalent cations (Mg^{2+}, Ca^{2+}), and trivalent cations (hexamine cobalt (III) and spermidine^{3+}) with λ-DNA-*Hind*III fragments ranging from 2,027 to 23,130 bp in Tris-borate-EDTA buffer solutions were examined using pulsed gel electrophoresis (Li et al., 1996, 1998; Holzwarth et al., 1989). The divalent or trivalent counterions competed with $Tris^+$ and Na^+ for binding onto polyion DNA, and the competition binding details were investigated by measuring the reduction of DNA gel electrophoretic mobility under a specific ion environment. The measured data were interpreted by the Henry gel model (Cantor and Schimmel, 1980; Rice and Nagasawa, 1961) and Manning's CC theory (Manning, 1977, 1978). Good agreement was found between the experimental data, based on mobility reduction measurements converted to the total charge neutralization fraction θ, and the predicted value from Manning's CC theory.

In our studies of counterion competition binding, the ionic strength, counterion valence, and DNA molecular weight effects on the competition binding were carefully investigated (Li et al., 1996, 1997, 1998). From these studies we developed an insight into the counterion binding system which revealed that the above phenomena could all be associated with an important parameter defined to be the iso-competition point [ICP] (Li et al., 1997). The ICP refers to a critical multivalent cation concentration, at a given ionic strength and temperature, where the multivalent cations possess a charge neutralization fraction on DNA equal to that of monovalent cations. In the following paper we discuss the definition and calculation of ICP, and how ICP may be applied to characterize and interpret the counterion competition binding. It will be shown that the ICP param-

Received for publication 9 November 1998 and in final form 16 March 1999.

Address reprint requests to Dr. Kenneth A. Marx, Department of Chemistry, University of Massachusetts Lowell, One University Ave., Lowell, MA 01854. Tel.: 978-934-3658; Fax: 978-934-3013; E-mail: Kenneth_Marx@uml.edu.

Dr. Li's present address is Genome Therapeutics Corporation, 100 Beaver Street, Waltham, MA 02453. E-mail: anzhi.li@genomecorp.com.

0006-3495/99/07/114/09 $2.00

eter actually presents a prospective picture of the counterion competition binding to polyelectrolyte DNA under a specific ion environment condition.

DEFINITION AND COMPUTATION

In this section we define ICP through three simultaneous equations that include Manning's two equations, and present the approach to calculate ICP corresponding to a specific ion environment.

Definition of ICP

The parameter ICP is closely associated with Manning's CC theory. In Manning's two-variable CC system, two species of counterions of different valences are present in solution to compete for binding to the polyion. Suppose in the solution the lower-valence cation is monovalent (the general case), and the higher-valence cations are one of the following: divalent, trivalent or tetravalent. In the above competition environment, θ_1 represents the fraction of charge neutralized by monovalent, and θ_Z is the number of Z-valent ions condensed per phosphate where the valence $Z = 2$, 3, or 4, respectively. $Z\theta_Z$ refers to the fraction of DNA charge neutralized by the divalent, trivalent, or tetravalent cations. To calculate the iso-competition point, another equation, Eq. 3, is added to Manning's original two equations (Manning, 1978; Wilson and Bloomfield, 1979). The three simultaneous equations are as follows:

$$1 + \ln(1000\theta_1/V_{p1}) = -2\xi(1-\theta_1-Z\theta_Z)\ln(1 - e^{-\kappa b}) \quad (1)$$

$$\ln(\theta_Z/C_Z) = \ln(V_{pZ}/1000e) + Z\ln(1000\theta_1 e/C_1 V_{p1}) \quad (2)$$

$$\theta_1 = Z\theta_Z \quad (3)$$

where C_1 and C_Z represent the molar concentration of monovalent and higher valence counterions. Similarly, V_{p1} and V_{pZ} represent the volume per mole phosphate where the condensed counterions (monovalent or higher valent) are considered to be territorially bound. The formula for calculating V_{pZ} is given in our previous publication (Li et al., 1998). The charge density parameter, ξ, is an important parameter in Manning's counterion condensation theory (Manning, 1978) which governs the counterion binding. The term b refers to the average axial charge spacing. Specifically, b = 1.7 Å and $\xi = 4.2$ at 25°C for double-stranded DNA in aqueous solution. κ is the Debye-Hückel screening parameter, which is itself dependent on the ionic strength (Cantor and Schimmel, 1980). The constant e refers to the base of natural logarithms.

Solving simultaneous Eqs. 1 and 2 iteratively, the charge neutralization fractions θ_1, and θ_Z, then the total charge neutralization fraction

$$\theta = \theta_1 + Z\theta_Z \quad (4)$$

can be obtained based on the following specific conditions of ion environment: the Debye-Hückel screening parameter κ (corresponding to a specific ionic strength) and the molar concentrations of competing cations, C_1 and C_Z. In general, $C_Z \ll C_1$, and the ionic strength contribution from the higher valence cation can be ignored relative to the ionic strength contribution from the monovalent, and thus the ionic strength of the system is close to the monovalent concentration C_1. For simplifying the ICP calculation, we assume the ionic strength remains constant when low concentrations of multivalent cation C_Z ($C_Z/C_1 < 0.01$) are added to the two-species system because its contribution to the ionic strength can be ignored. For a fixed ionic strength and C_1, each multivalent concentration C_Z corresponds to a pair of predicted charge neutralization fraction values θ_1 and θ_Z, and then total charge neutralization fraction θ based on Eq. 4.

Unlike the case of solving Manning's two variable equations, the higher valence cation concentration C_Z becomes a variable to be determined, instead of a known one. Only one pair of charge neutralization fraction data (θ_{1_ICP} and θ_{Z_ICP}) among all infinite pairs (θ_1 and θ_Z) will be selected to satisfy Eq. 3 when the ionic strength C_1 and temperature are fixed. The multivalent cation concentration C_{Z_ICP} along with θ_{1_ICP} and θ_{Z_ICP} are the three solutions for the simultaneous Eqs. 1–3 corresponding to a fixed ionic strength C_1 and temperature. C_{Z_ICP} is defined to be the iso-competition point (ICP). At this critical multivalent cation concentration, ICP, the two rival monovalent, and multivalent cation competitors possess an equal binding fraction of the polyion DNA charge.

Computation of ICP

To obtain the value of ICP where Eqs. 1–3 need to be solved simultaneously, the MATHEMATICA tool (Wolfram, 1991) was employed to execute the iterative numerical calculations, and the computation approach is similar to that described in the following publications (Li et al., 1996, 1998). The main procedure is divided into two steps: calculation of the ion environment and simultaneous solution of the three equations.

If the calculation of ICP is associated with a particular experimental environment, it is necessary in the first step to analyze the ion environment and calculate the correct ionic strength and monovalent cation concentration as well. The ionic strength is calculated corresponding to a particular ion environment based on the Henderson-Hasselbalch equation (Perrin and Dempsey, 1979) where the pK_a value was corrected iteratively using the Davies equation (Perrin and Dempsey, 1979) to be pK_a', corresponding to the chosen ionic strength. If ICP calculation is not associated with a real experimental system, but is a simulation, the first step could be skipped. In the simulation system, the ionic strength value could be set equal to the monovalent concentration.

For the second step, obtaining the numerical solutions of the three simultaneous equations, the Debye-Hückel screening parameter κ should be calculated according to the

known ionic strength (Li et al., 1996). The condensation volumes V_{p1}, V_{p2}, V_{p3}, and V_{p4} then need to be computed corresponding to the individual valences $Z = 1, 2, 3, 4$, respectively (Li et al., 1998). With all parameters substituted in Eqs. 1–3, these simultaneous equations are solved iteratively by a small program based on the MATHEMATICA tool (Wolfram, 1991). The specific charge neutralization fractions θ_{1_ICP} and θ_{Z_ICP} and the critical multivalent cation concentration ICP were obtained. At this particular ICP we have the following relationship: $\theta_{1\_ICP} = Z\theta_{Z\_ICP}$, which states the concept of the ICP mathematically. It illustrates that the DNA charge neutralized by the monovalent cation θ_{1_ICP} is equal to that neutralized by the higher valence cation, which is $Z\theta_{Z\_ICP}$.

PROPERTIES of ICP

In this section we present and discuss important features of the calculated ICP values to have an essential understanding of the nature of ICP.

Iso-charge neutralization line

Fig. 1 maps the logarithm (ICP) versus total charge neutralization fraction θ_{ICP}. Three curves, representing the respective divalent, trivalent, and tetravalent cases, where the monovalent counterion competes with the higher valence ions ($Z = 2, 3, 4$), are presented. When calculating the ICPs in Fig. 1, the ionic strength was assumed to be equal to the monovalent concentration C_1, and the temperature was set to 23°C. The ionic strength ranges from 1 to 75 mM, which covers a wide range of ionic strengths appropriate to practical applications. Meanwhile, the ICP range is 0.175 μM to 0.95 mM for divalent, 5.08×10^{-5} to 20 μM for trivalent, and 2.3×10^{-7} to 0.5 μM for tetravalent. The horizontal lines drawn in Fig. 1 are iso-charge neutralization lines.

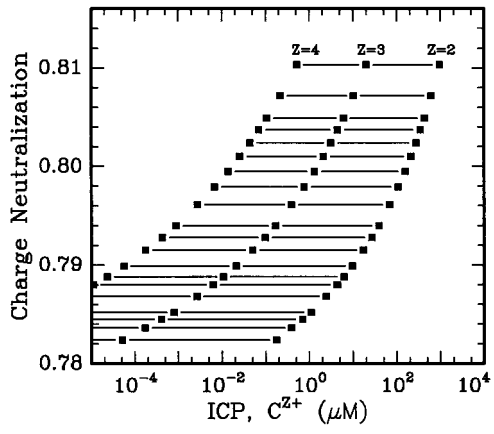

FIGURE 1 Logarithm of ICP versus total charge neutralization θ. Three sets of points from right to left represent the ICP_{di}, ICP_{tri}, and ICP_{tetra}, respectively. The horizontal lines are iso-charge neutralization lines corresponding to a specific ionic strength. The range of ionic strength represented by points from bottom to top is 1–75 mM.

Each line connects the ICPs for divalent, trivalent, and tetravalent cations versus total charge neutralization fraction. The series of iso-charge neutralization lines presented from bottom to top corresponds to different ionic strengths in the range 1–75 mM, respectively. It is clear from these data that when cation valence changes, ICP values change dramatically, but the total charge neutralization fraction θ_{ICP} remains constant for a specific ionic strength condition. However, the iso-charge neutralization lines demonstrate that regardless of cation valence, when the competition reaches the equivalence point (ICP), where the charge neutralization fraction is equal from higher valence and monovalent cations, the total charge neutralization fraction θ_{ICP} is constant for a specific ion environment.

The iso-charge neutralization line can be proved theoretically. Based on Eqs. 3 and 4, we have:

$$\theta_{ICP,di} = \theta_{1\_ICP} + 2\theta_{2\_ICP} = 2\,\theta_{1\_ICP} \tag{5A}$$

$$\theta_{ICP,tri} = \theta_{1\_ICP} + 3\theta_{3\_ICP} = 2\,\theta_{1\_ICP} \tag{5B}$$

$$\theta_{ICP,tetra} = \theta_{1\_ICP} + 4\theta_{4\_ICP} = 2\,\theta_{1\_ICP} \tag{5C}$$

where $\theta_{ICP,di}$, $\theta_{ICP,tri}$, and $\theta_{ICP,tetra}$ refer to the total charge neutralization at ICP where the multivalent cation is divalent, trivalent, and tetravalent, respectively. The right sides $2\,\theta_{1\_ICP}$ in Eqs. 5, A–C are equal since ionic strengths are the same. The iso-charge neutralization equation then could be expressed as:

$$\theta_{ICP,di} = \theta_{ICP,tri} = \theta_{ICP,tetra} = \theta_{ICP} \tag{5D}$$

Notice that the total charge neutralization θ_{ICP} in Fig. 1 slowly rises with increasing ionic strength.

Semi-quantitative equations

ICP values change when valence or ionic strength changes. In Fig. 1, ICP values decrease dramatically when valence increases, and the relationship $ICP_{di} \gg ICP_{tri} \gg ICP_{tetra}$ is always observed. For example, in a two-species system of 20 mM ionic strength, ICP_{di} equals 68.81 μM for divalent cations, ICP_{tri} is 0.39 μM for trivalents, and ICP_{tetra} is 2.755×10^{-3} μM for tetravalents. It is not surprising to see the ICP change so dramatically versus valence if one considers Manning's two-variable CC theory. As we might expect, this ICP valence phenomenon is somewhat similar to the valence effect of CC theory.

Below we present the semiquantitative equations to describe the ICP value dependence on two variables, valence Z and ionic strength I, based on a curve-fitting approach. Fig. 2 shows the relationship between ICP and ionic strength, for monovalent counterions competing with divalent cations in Fig. 2 *A*, trivalent cations in Fig. 2 *B*, and tetravalent cations in Fig. 2 *C*. The three best-fit equations obtained from the curve-fitting shown in the figures can be written in a generalized form as:

$$ICP_Z = Const_Z I^Z \tag{6A}$$

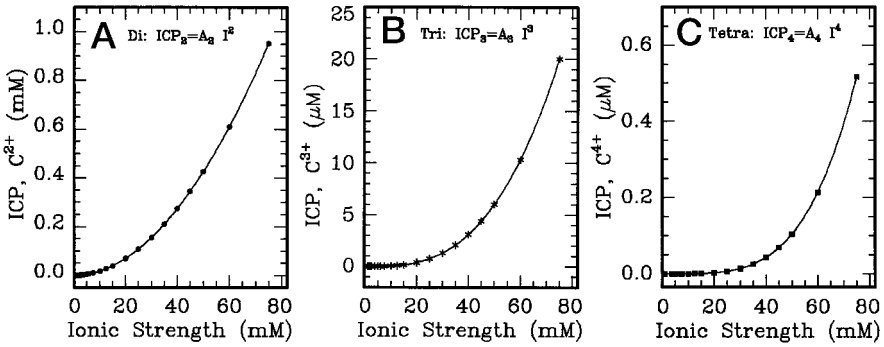

FIGURE 2 Relationship of ICP versus ionic strength where the higher-valence cation is: (*A*) divalent, (*B*) trivalent, and (*C*) tetravalent, respectively. Curve fits through the calculated points are of the type described in each panel.

and

$$\mathrm{ICP_{Za}}/\mathrm{ICP_{Zb}} = (I_a/I_b)^Z \qquad (6B)$$

ICP and CCP

In studying the condensation-based collapse of DNA, it is well known that reaching a critical charge neutralization fraction (0.890) of the DNA is required to bring about the DNA collapse (Wilson and Bloomfield, 1979). The critical collapse conditions were described (Li et al., 1996) by C_1, where ionic strength equals C_1, and the critical collapse point (CCP) defined as the trivalent cation concentration. Fig. 3 *A* presents curves of ICP and CCP versus ionic strength, where $I = C_1$. At a fixed temperature, each ionic strength has an ICP value, where the counterion competition binding reaches a balance and the charge neutralization fraction is equal from the competing monovalent and trivalent counterions. Also, each ionic strength has a CCP, where the total charge neutralization fraction is 0.890. It is clear that at any ionic strength the CCP value is much higher than ICP. That is because ICP is a transition point where the trivalent counterions start to dominate the binding to DNA, and CCP is the "final" point where the charge neutralization fraction caused mainly by trivalent counterions finally brings about the conformational collapse of DNA. In Fig. 3 *B* the nonlinear relationship between CCP and ICP is observed. The slope of the curve is lower when ionic strength increases in Fig. 3 *B*, which corresponds to the decreasing distance between ICP and CCP points when ionic strength rises in Fig. 3 *A*. This is the case because at higher ionic strength the total charge neutralization, θ_{ICP}, has a higher value, which is closer to the critical charge neutralization fraction of 0.890.

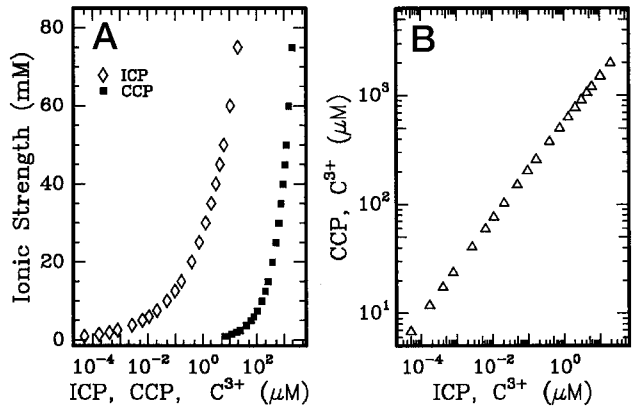

FIGURE 3 (*A*) Logarithm of ICP and CCP versus ionic strength. CCP is the critical collapse point, corresponding to a total charge neutralization of DNA of 0.890, which will bring about the tertiary structure collapse of DNA to insoluble toroidal self-assembled structures. (*B*) Relationship between the logarithm of CCP and ICP.

INTERPRETATION OF COUNTERION BINDING BY ICP

The concept of ICP is closely associated with Manning's two-variable CC theory, and it is introduced to characterize and interpret the counterion competition binding in the two-species system.

ICP and valence effects

In Fig. 4 the charge neutralization fraction from monovalent θ_1, from multivalent θ_2, (θ_3) and the total θ versus the logarithm of multivalent ion concentration C_2 (C_3) is presented. Notice that the heavy symbols represent the trivalent case and the light symbols represent the divalent case. The data of Fig. 4 were calculated by CC theory to correspond to two separate competition binding systems we have experimentally investigated. One is the binding of $Co(NH_3)_6^{3+}$ to λ-DNA-*Hind*III fragments in 22.79 mM ionic strength and 19.80 mM monovalent ion concentration; another is the binding of Mg^{2+} to λ-DNA-*Hind*III fragments in 17.70 mM ionic strength and 17.67 mM monovalent ion concentration. The theoretical curves show the competition binding between divalent and trivalent cations with monovalent cations directly. Upon inspection of trivalent cations (0.01–400 μM) competing with monovalent cations (19.80 mM) in an ionic strength of 22.79 mM, one notices that the monovalent charge fraction drops rapidly, whereas the trivalent cation charge fraction rises at the same rate, and the two curves cross at 0.387 μM, where trivalent and monovalent cations have equal charge neutralization fractions. Under these conditions the trivalent cation concentration

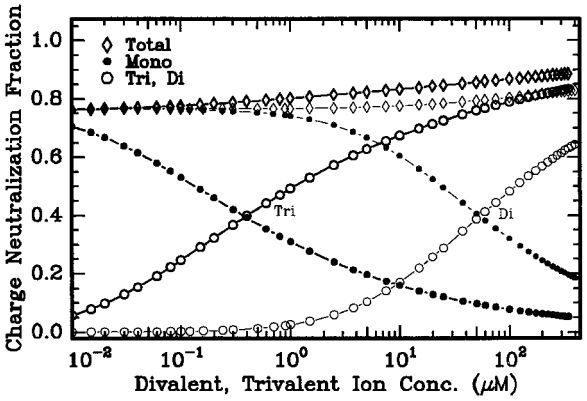

FIGURE 4 Valence effect on DNA charge neutralization fractions θ_1, $2\theta_2$, ($3\theta_3$), and θ, calculated by CC theory versus logarithm of divalent or trivalent cation concentration under similar ionic conditions. For trivalent cations the ionic strength is 22.79 mM and C_1 = 19.80 mM, while for divalent cations the ionic strength is 17.70 mM and C_1 = 17.67 mM. Note that the light symbols indicate the divalent versus monovalent competition system, and the heavy symbols indicate the trivalent versus monovalent competition system.

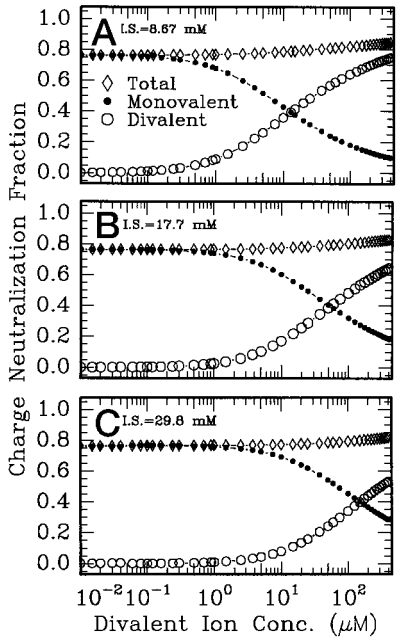

FIGURE 5 Ionic strength effect on charge neutralization fractions θ_1, $2\theta_2$, and θ, calculated by CC theory. The θ_1, $2\theta_2$, and θ versus logarithm of divalent cation concentration is presented under the following ionic conditions: (*A*) 8.67 mM ionic strength and 8.65 mM monovalent ion concentration; (*B*) 17.70 mM ionic strength and 17.67 mM monovalent ion concentration; (*C*) 29.78 mM ionic strength and 29.73 mM monovalent ion concentration. Curves represented by solid circle, open circle, and diamond symbols indicate the charge neutralization fraction θ_1, $2\theta_2$, and θ, respectively.

0.387 μM is nothing but the ICP. After this point the trivalent cation dominates the binding competition. In the case of divalent cations (0.01–400 μM) competing with monovalent cations (17.67 mM) in an ionic strength of 17.70 mM, a different quantitative binding behavior is observed. The rising rate of charge neutralization fraction θ_2 is much slower than θ_3 in the previous case, and the same is true of the decreased rate of θ_1 lowering. The divalent cation concentration (ICP) corresponding to the crossover point is 53.70 μM where divalent and monovalent cations have equal charge neutralization fractions. Notice that the ICP of divalent cations is much larger (more than two orders of magnitude) than ICP of trivalent cations under very similar ion environment conditions. Knowing the values of ICP (divalent and trivalent), one can evaluate how rapidly the trivalent cation will dominate the DNA binding competition in contrast to the much less effective divalent cation competitor. The valence effect on competition binding reflected by ICP here is consistent with the valence behavior of ICP shown in Fig. 1. It is clear that the ICP parameter provides an important reference point for viewing a competition binding system, and indeed these data may help to design binding experiments.

ICP and ionic strength effect

The ionic strength effect on counterion binding has been discussed thoroughly in previous publications (Li et al., 1996, 1998). Here we intend to characterize the ionic strength effect on counterion binding using the novel parameter ICP. Fig. 5 presents charge neutralization fraction θ_1, θ_2 and θ versus the logarithm of divalent cation concentration at three different ionic strengths that correspond to experimental data from Li et al., 1998. The theoretical curves were calculated by CC theory. The competition conditions in Fig. 5, *A–C*, are divalent cations [Mg^{2+}] (0.01–400 μM) competing with monovalent cation [Na^+, $Tris^+$] at concentrations of 8.65 mM, 17.67 mM, and 29.73 mM binding to λ-DNA-*Hind*III fragments at ionic strengths of 8.67 mM, 17.70 mM, and 29.78 mM, respectively. It is observed that the crossover point, where charge neutralization from monovalent cation θ_1 is equal to that from divalent $2\theta_2$, shifts to the right when ionic strength increases. The ICP values, where divalent cation concentration C_2 corresponds to the crossover point values, are 12.98, 53.70, and 150 μM in Fig. 5, *A–C*, respectively. The above ICP values characterize the ionic strength effect. The higher the ionic strength, the larger the ICP, which indicates that a higher divalent cation concentration is required to reach the point where it can start to dominate the binding. Quantitatively, one can use Eq. 6 B: $ICP_{Za}/ICP_{Zb} = (I_a/I_b)^Z$, where $Z = 2$, to test the above data. Using our ICP data we have 53.70 μM/12.98 μM = 4.14, and for ionic strength (17.70 mM/8.67 mM)^2 = 4.16. The small difference in these two values may be caused by using limited significant digits in these calculations or it may be due to the necessity for another constant added to Eq. 6 A, as $ICP_Z = Const_Z\, I^Z +$ Const. Nonetheless, Eqs. 6 A and B are useful to predict an unknown ICP from a given ICP and the ratio of the known ionic strengths.

ICP and DNA size effect

Previous investigations (Li et al., 1997, 1998) reveal that the experimental data collected by pulsed gel electrophoresis shows a distribution of normalized mobility μ/μ_o or converted charge neutralization fraction θ over the range of DNA lengths from 2.0 to 23.1 kbp. The larger the fragment length, the higher the total charge neutralization fraction. It was observed that the distribution of $\Delta(\mu/\mu_o)$ was dependent on the ionic strength, cation valence, and multivalent cation concentration. Fig. 6 presents the normalized mobility μ/μ_o versus divalent Ca^{2+} concentration at different ionic strengths (I = 4.84, 15.0, 20.2, and 25.4 mM). The agreement between experimental measurements (*symbols*) and CC prediction (*solid line*) is good. Also, a consistent DNA length effect on μ/μ_o associated with the ionic strength was observed. The relative shift $\Delta(\mu/\mu_o)/(\mu/\mu_o)$ was calculated by subtracting the μ/μ_o of the largest fragment (f_1) from that of the smallest (f_6) and normalizing the difference by the μ/μ_o value of f_6. The $\Delta(\mu/\mu_o)/(\mu/\mu_o)$ "shift" increased with increasing C_2 and decreasing ionic strength. It is obvious to see that the shift phenomenon can be ignored in Fig. 6 *D*, which corresponds to a higher ionic strength, while the shift phenomenon is strongest in Fig. 6 *A*, which corresponds to the lowest ionic strength. The study of Li and Marx, 1997 demonstrates that the shift phenomenon only occurs when divalent concentration C_2 is high enough to dominate the competition binding, which is measured by comparing C_2 to the ICP, and ICP itself is ionic strength-dependent.

Fig. 7 *A* is a survey plot that includes four columns: ionic strength (I), ICP, Ca^{2+} concentration, and shift $\Delta(\mu/\mu_o)/(\mu/\mu_o)$. The three factors ($I$, ICP, Ca^{2+} concentration) govern the shift $\Delta(\mu/\mu_o)/(\mu/\mu_o)$ magnitude. The value of each variable is represented by the width of the corresponding rectangle. The first column shows four ionic strengths, the second column shows four ICP values corresponding to the four ionic strengths. In the third column, the concentration of Ca^{2+} was represented by three rectangles: 10, 20, 40 μM for each ionic strength and ICP values. The fourth column shows the measured relative shift $\Delta(\mu/\mu_o)/(\mu/\mu_o)$ associated with the particular horizontal row of I, ICP, and Ca^{2+} conditions. ICP is the key to the connection between measured shift $\Delta(\mu/\mu_o)/(\mu/\mu_o)$ and the controlling factors (I, ICP, Ca^{2+} concentration) in Fig. 7 *A*. When the Ca^{2+} concentration is larger than or close to its ICP where the divalent cations dominate the competition binding, the shift $\Delta(\mu/\mu_o)/(\mu/\mu_o)$, which is a function of DNA length and the ion environment, is measurable. Because the divalent counterion condensation brings about a conformation change of the DNA fragments, this could result in an end-to-end distance decrease that is length-dependent (Li et al., 1997). For example, in the case of 4.8 mM ionic strength, the Ca^{2+} concentrations (10, 20, 40 μM) are all larger than ICP (4.1 μM) and the shifts are all observable. Obviously, when the Ca^{2+} concentration equals 40 μM, the maximum shift is shown both in Fig. 7 *A* and Fig. 6 *A*. By contrast, when the ionic strength equals 25.4 mM and the ICP is high (111.3 μM), the divalent Ca^{2+} concentrations (10, 20, 40 μM) are all smaller than ICP and the shift (1%) magnitude can be ignored.

DISCUSSION

Visualizing competition binding and ICP

In this paper we introduce an important parameter, the iso-competition point (ICP), to characterize the competition binding in a two-species system. By imposing the condition of charge neutralization equivalence $\theta_1 = Z\theta_Z$ upon Man-

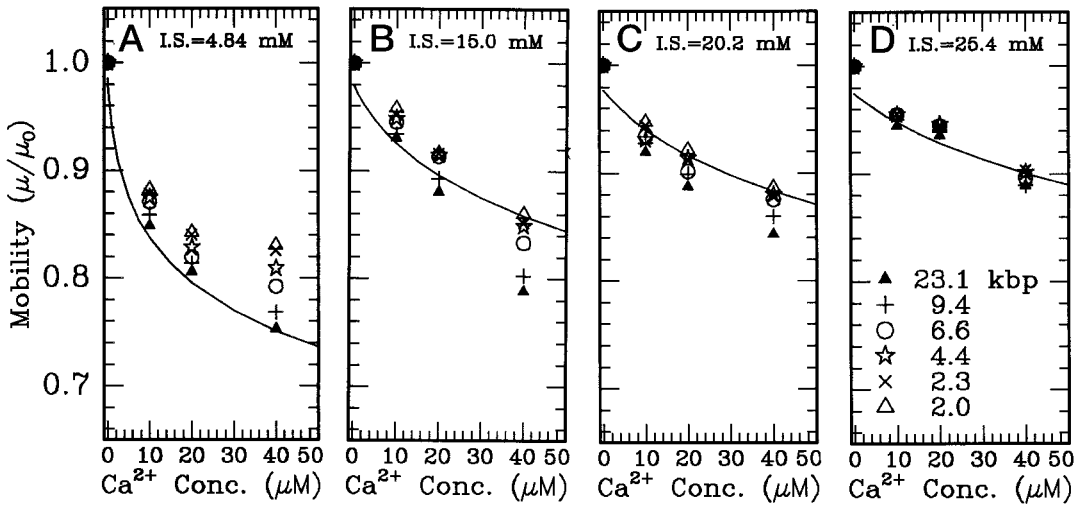

FIGURE 6 Normalized mobility μ/μ_0 of λ-DNA-*Hind*III fragments versus Ca^{2+} concentration under the following ionic conditions: (*A*) 4.84 mM ionic strength and 4.83 mM monovalent ion concentration; (*B*) 14.97 mM ionic strength and 14.95 mM monovalent ion concentration; (*C*) 20.18 mM ionic strength and 20.14 mM monovalent ion concentration; (*D*) 25.43 mM ionic strength and 25.38 mM monovalent ion concentration. The experimental data for different molecular weight bands represented by the symbols were fit by Manning's CC theory, shown by the solid lines.

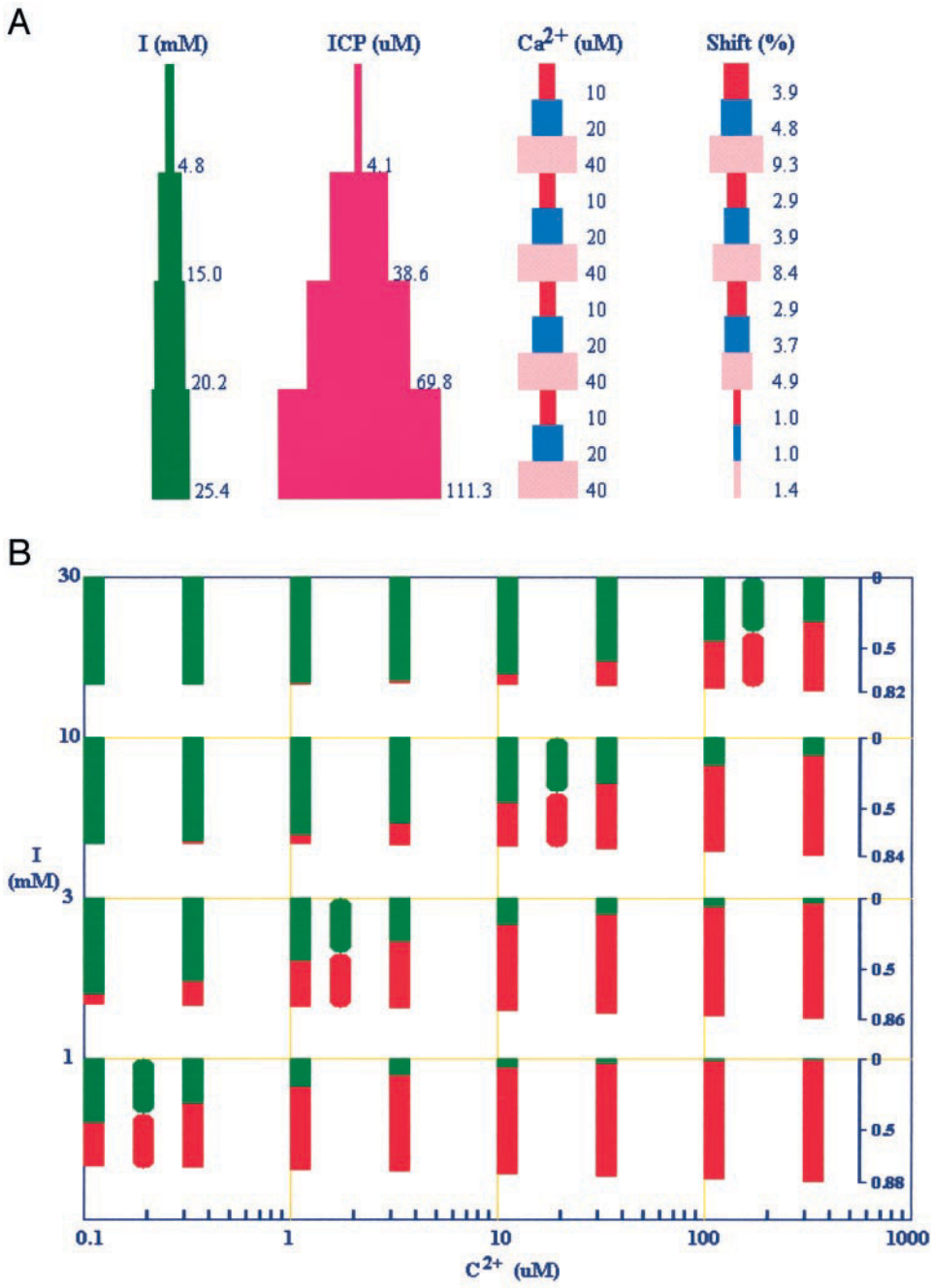

FIGURE 7 Visualizations of competition binding and ICP. (*A*) Survey plot of the interrelationship among ionic strength *I*, ICP, Ca^{2+} concentration, and relative mobility shift $\Delta(\mu/\mu_o)/(\mu/\mu_o)$. Ionic strength, ICP, Ca^{2+} concentration, and measured shift values $\Delta(\mu/\mu_o)/(\mu/\mu_o)$ are "listed" in four columns. The value of each parameter is represented by the width of the corresponding rectangle. It is shown that the occurrence of a significant shift is dependent on whether the ratio of Ca^{2+} concentration to ICP is larger than or close to 1 for the solution conditions corresponding to any horizontal row of the table. (*B*) Icon graph mapping competition binding and iso-competition points. The logarithm of divalent cation concentration (*x* axis) and logarithm of ionic strength (*y* axis) locates the icon in the graph. A rectangular icon is used to present three parameters by its color and volume. The green portion of the rectangle refers to the charge fraction θ_1 neutralized by monovalent cations, the red portion of the rectangle refers to the charge fraction $2\theta_2$ neutralized by divalent cations, and the total volume of the rectangle indicates the total charge neutralization fraction θ. The round-edged rectangular icon is used to present charge fractions of ICP whose green and red charge fraction portions are exactly equal ($\theta_1 = 2\theta_2$). Notice that at one ionic strength (one horizontal row), only one ICP exists.

ning's two simultaneous equations, ICPs can be calculated, each corresponding to a specific ionic strength. With the help of Fig. 7 *B* we review the ICP concept and its connection with Manning's CC theory in a visual way.

Fig. 7 *B* is an icon graph (Pickett and Grinstein, 1988) drawn using visualization techniques (Nielson et al., 1997) and Java programing (Campione and Walrath, 1997). Instead of a point located in a coordinate system in the traditional scatter plot, an icon is used to present multiple variables in a 2-D plot. A rectangular icon is chosen to present three variables by color and volume. The green portion of each rectangle refers to the charge fraction θ_1 neutralized by monovalent cations. The red portion of the rectangle refers to the charge neutralization fraction $2\theta_2$, and the total volume of the rectangle indicates the total charge neutralization fraction θ. A logarithm coordinate system was chosen to locate the icons in the ion environment comprised of the ionic strength (*y* axis) and divalent cation concentration (*x* axis). The ionic strength, where $I = C_1$, covers the practical range of 1–30 mM, while at each ionic strength, Ca^{2+} varies over the range of 0.1 to 300 μM. At a given ionic strength, upon scanning the graph from left to right, it is clear that the green portion of successive icons is gradually decreasing, while the red portion is increasing with rising divalent cation concentration. There is a special icon whose shape is rounded at the edges and its green

portion exactly equals the red portion. This special icon signifies the charge neutralization fraction of ICP and the value of ICP at a particular divalent cation concentration. Notice that for one ionic strength, only one ICP exists and the special icon shows the ion competition balance visually. All the icons located on the left side of the ICP icon have larger green portions than red ones, while all the icons located on the right side of the ICP icon have larger red portions than green ones. It is clearly shown that the ICP represents a transition point, after which the divalent cations dominate the counterion binding, and the charge on polyion DNA is mostly neutralized by the divalent cations. Upon viewing the graph from bottom to top and from left to right simultaneously, the ionic strength effect will be clear. The icons in the bottom row with the lowest ionic strength (1 mM) have green portions decreasing rapidly with the increase of divalent cation concentration. It reveals at the low ionic strength that divalent cations strongly compete with the monovalent cations. Even at very low Ca^{2+} concentration they dominate the competition binding, and the position of the ICP icon is located at low divalent cation concentration. For the top row with the highest ionic strength (30 mM) the competition picture is reversed, and the ICP icon appears at very high cation concentration. When viewing the icons by rows, 12 "curves" are shown. Three curves can be viewed in each horizontal row corresponding to one ionic strength. The θ_1 curve is represented by the green rectangle; the $2\theta_2$ curve represented by the red rectangle; and the θ curve is represented by the entire icon including green and red rectangles, which slowly increases with the increase in Ca^{2+}.

SUMMARY

The important points are summarized as follows:

1. Under fixed ionic strength condition (assume monovalent $C_1 = I$), only one ICP exists where the charge neutralization fraction on DNA from monovalent cations equals that from multivalent cations. That is, $\theta_{1\_ICP} = Z\theta_{Z\_ICP}$;
2. For fixed ionic strength, the total charge neutralization fractions θ_{ICP} are the same at ICP, no matter whether the higher valence cation is divalent, trivalent, or tetravalent. That is, $\theta_{ICP,di} = \theta_{ICP,tri} = \theta_{ICP,tetra} = \theta_{ICP}$;
3. The ionic strength effect on ICP could be expressed as $ICP_{Za}/ICP_{Zb} = (I_a/I_b)^Z$; this relationship can be viewed in the first and second column in Fig. 7 *A*, and the numbers fit the equation nicely;
4. The valence effect on ICP is very strong, but so far it hasn't been quantitatively expressed;
5. ICP is able to interpret and characterize the ionic strength, valence, and DNA length effects of the counterion competition binding in a two-species system;
6. Since we are discussing counterion condensation, where only territorially bound counterions fit Manning's CC theory, it is only these ions for which the ICP concept is relevant. For example, the transition metal cations such as Cu^{2+} and Zn^{2+} are known to bind strongly to the DNA nitrogenous bases rather than phosphate groups; they should not be treated using the ICP concept (Li et al., 1998).

We thank Prof. G. Manning for his insightful reading of our manuscript and Haiyan Huang for her biophysical experimental support.

The authors acknowledge support from the Center for Intelligent Biomaterials.

REFERENCES

Allison, S. A., J. C. Herr, and J. M. Schurr. 1981. Structure of viral φ 29 DNA condensed by simple triamines: a light-scattering and electron-microscopy study. *Biopolymers*. 20:469–488.

Arscott, P. G., A. Z. Li, and V. A. Bloomfield. 1990. Condensation of DNA by trivalent cations. 1. Effects of DNA length and topology on the size and shape of condensed particles. *Biopolymers*. 30:619–630.

Bloomfield, V. A. 1991. Condensation of DNA by multivalent cations: consideration on mechanism. *Biopolymers.* 31:1471–1481.

Campione, M., and K. Walrath. 1997. The Java Tutorial, Object-Oriented Programming for the Internet. Addison-Wesley, Reading, MA.

Cantor, C. R., and P. R. Schimmel. 1980. Biophysical Chemistry. Part II. Techniques for the Study of Biological Structure and Function. W. H. Freeman and Co., San Francisco.

Granot, J., and D. R. Kearns. 1982. Interactions of DNA with divalent metal ions. III. Extent of metal binding: experiment and theory. *Biopolymers*. 21:219–232.

Holzwarth, G., K. J. Platt, C. B. Mckee, R. W. Whitcomb, and G. D. Crater. 1989. The acceleration of linear DNA during pulsed-field gel electrophoresis. *Biopolymers*. 28:1043–1058.

Labarbe, R., S. Flock, C. Maus, and C. Houssier. 1996. Polyelectrolyte counterion condensation theory explains differential scanning calorimetry studies of salt-induced condensation of chicken erythrocyte chromatin. *Biochemistry*. 35:3319–3327.

Langlais, M., H. A. Tajmir-Riahi, and R. Savoie. 1990. Raman spectroscopic study of the effects of Ca^{2+}, Mg^{2+}, Zn^{2+} and Cd^{2+} ions on calf thymus DNA: binding sites and conformational changes. *Biopolymers*. 30:743–752.

Li, A. Z., T. Fen., and M. Din. 1992. Formation study of toroidal condensation of DNA. *Sci. China (Ser. B)*. 35:169–175.

Li, A. Z., H. Huang, and K. A. Marx. 1997. DNA end-to-end distance change due to divalent counterion condensation studied by pulse gel electrophoresis. *In* Statistical Mechanics in Physics and Biology. *MRS. Symposium Proceedings Series*. 463:67–72.

Li, A. Z., H. Huang, X. Re, L. J. Qi, and K. A. Marx. 1998. A gel electrophoresis study of the competitive effects of monovalent counterion on the extent of divalent counterions binding to DNA. *Biophys. J.* 74:964–973.

Li, A. Z., L. J. Qi, H. H. Shih, and K. A. Marx. 1996. Trivalent counterion condensation on DNA measured by pulse gel electrophoresis. *Biopolymers*. 38:367–376.

Ma, C., and V. A. Bloomfield. 1995. Gel electrophoresis measurement of counterion condensation on DNA. *Biopolymers.* 35:211–216.

Manning, G. S. 1977. Limiting laws and counterion condensation in polyelectrolyte solutions. IV. The approach to the limit and the extraordinary stability of the charge fraction. *Biophys. Chem.* 7:95–102.

Manning, G. S. 1978. The molecular theory of polyelectrolyte solutions with applications to the electrostatic properties of polynucleotides. *Q. Rev. Biophys.* 11:179–246.

Manning, G. S. 1981. Limiting laws and counterion condensation in polyelectrolyte solutions. 7. Electrophoretic mobility and conductance. *J. Phys. Chem.* 85:1508–1515.

Manzini, G., L. E. Xodo, F. Fogolari, and F. Quadrifoglio. 1990. Secondary structure effects on the interaction of different polynucleotides with Ca^{2+}. *Biopolymers.* 30:325–333.

Marx, K. A., and T. C. Reynolds. 1982. Spermidine-condensed phix-174 DNA cleavage by micrococcal nuclease: torus cleavage model and evidence for unidirectional circumferential DNA wrapping. *Proc. Natl. Acad. Sci. USA*. 79:6484–6488.

Marx, K. A., and T. C. Reynolds. 1989. Micrococcal nuclease digestion study of spermidine-condensed DNA. *Int. J. Biol. Macromol.* 11: 241–248.

Marx, K. A., and G. C. Ruben. 1983. Evidence for hydrated spermidine-calf thymus DNA toruses organized by circumferential DNA wrapping. *Nucleic Acids Res.* 11:1839–1854.

Marx, K. A., and G. C. Ruben. 1986. A study of phix-174 DNA torus and λ DNA torus tertiary structure and the implications for DNA self-assembly. *J. Biomol. Struct. & Dyn.* 4:23–29.

Nielson, G. M., H. Hagen, and H. Müller. 1997. Scientific Visualization, Overviews, Methodologies, and Technologies. IEEE Computer Society Press, Los Alamitos, CA.

Perrin, D. D., and B. Dempsey. 1979. Buffers for pH and Metal Ion Control. Chapman and Hall, London.

Pickett, R. M., and G. G. Grinstein. 1988. Iconographics displays for visualizing multidimensional data. *Proceedings of the IEEE Conference on Systems, Man, and Cybernetics, PRC, Beijing and Shenyang*. 514–519.

Plum, G. E., P. G. Arscott, and V. A. Bloomfield. 1990. Condensation of DNA by trivalent cations. 2. Effects on cation structure. *Biopolymers.* 30:631–643.

Rhee, K. W., and B. R. Ware. 1983. DNA-divalent metal cation interactions measured by electrophoretic light scattering. *J. Chem. Phys.* 78: 3349–3353.

Rice, S. A., and M. Nagasawa. 1961. Polyelectrolyte Solutions. Academic Press, New York.

Widom, J., and R. L. Baldwin. 1980. Cation-induced toroidal condensation of DNA studies with $Co^{3+}(NH_3)_6$. *J. Mol. Biol.* 144:431–453.

Wilson, R., and V. A. Bloomfield. 1979. Counterion-induced condensation of deoxyribonucleic acid. A light-scattering study. *Biochemistry*. 18: 2192–2196.

Wolfram, S. 1991. Mathematica. A system for doing mathematics by computer. Addison-Wesley Publishing Co., Reading, MA.

Xia, J., P. L. Dubin, and H. A. Havel. 1993. Electrophoretic light scattering study of counterion condensation on polylysine. *Macromolecules.* 26: 6335–6337.